J Fluoresc (2010) 20:135–142
DOI 10.1007/s10895-009-0531-6

ORIGINAL PAPER

Photophysics of 2-(4′-*N*,*N*-Dimethylaminophenyl)imidazo [4,5-b]pyridine in Micelles: Selective Dual Fluorescence in Sodium dodecylsulphate and Triton X-100

Nihar Dash · G. Krishnamoorthy

Received: 27 March 2009 / Accepted: 7 August 2009 / Published online: 21 August 2009

Abstract The photophysical behavior of 2-(4′-*N*,*N*-dimethylaminophenyl)imidazo[4,5-b]pyridine (DMAPIP-b) has been studied in nonionic triton X-100 (TX-100), cationic cetyltrimethylammonium bromide (CTAB) and anionic sodium dodecylsulfate (SDS) micelles using steady state and time resolved fluorescence techniques. The molecule emits both normal and TICT fluorescence in SDS and TX-100 but emits only normal fluorescence in CTAB. This difference in behavior of the fluorophore is due to varying extent of hydrogen bonding experience by it in different micelles. Of the three possible monocations, only two kinds of monocations, MC1 (formed by protonation of pyridine ring nitrogen) and MC2 (formed by the protonation of imidazole nitrogen) are present in all the micelles (Scheme 1). DFT calculations performed on the monocations reveal that MC1 and MC2 are more stable than MC3, the monocation formed by the protonation of dimethylamino nitrogen.

Keywords TICT · Fluorescent probe · Prototropic equilibrium · Hydrogen bonding

Introduction

Molecules those emit intramolecular charge transfer (ICT) fluorescence have attracted growing interest in recent investigations [1, 2]. When excited, the fluorophore could give a dual fluorescence due to emission from both the locally excited (LE) state and the twisted intramolecular charge transfer (TICT) state. This dual fluorescence emission is very sensitive to polarity and viscosity [1, 2]. Thus TICT compounds are important for applications, for example, as a fluorescence sensor and as a probe and in material science [3, 4].

In our recent communication [5], we have reported the protic solvent induced dual fluorescence emission of 2-(4′-*N*, *N*-dimethylaminophenyl)imidazo[4,5-b]pyridine (DMAPIP-b, Scheme 1). The longer wavelength emission is due to formation of the TICT state facilitated by hydrogen bonding of the solvent with the pyridine nitrogen. The TICT fluorescence increases with increasing hydrogen bond donating capacity and polarity of the solvent, but no dual fluorescence was observed in water. The TICT fluorescence also decreases with increase in viscosity of medium. Thus the dual fluorescence emission of DMAPIP-b is expected to be modulated by viscosity, polarity and hydrogen bonding capacity of the environment.

The study of micellar solutions is of interest both from the point of view of basic research and applications of surfactants. Micelles also simulate a more complex environmental conditions present in larger bioaggregates such as membranes. Therefore micelles are being extensively studied as rudimentary models for biological lipid membrane systems [6, 7]. Attention has been paid to the micellar activities on the nature and characteristics of different photophysical and photochemical processes [4, 5, 8, 9]. Upon binding, a molecule will experience a different environment inside the microheterogeneous structure of micelle, than that of bulk solvents for e.g., polarity, viscosity and diffusion of water molecules changes on moving towards the core of the micelle. In other words, the micelles can influence the TICT emission of DMAPIP-b in a unique way. Thus we have investigated the effects

N. Dash · G. Krishnamoorthy (✉)
Department of Chemistry,
Indian Institute of Technology Guwahati,
Guwahati 781039, India
e-mail: gkrishna@iitg.ernet.in

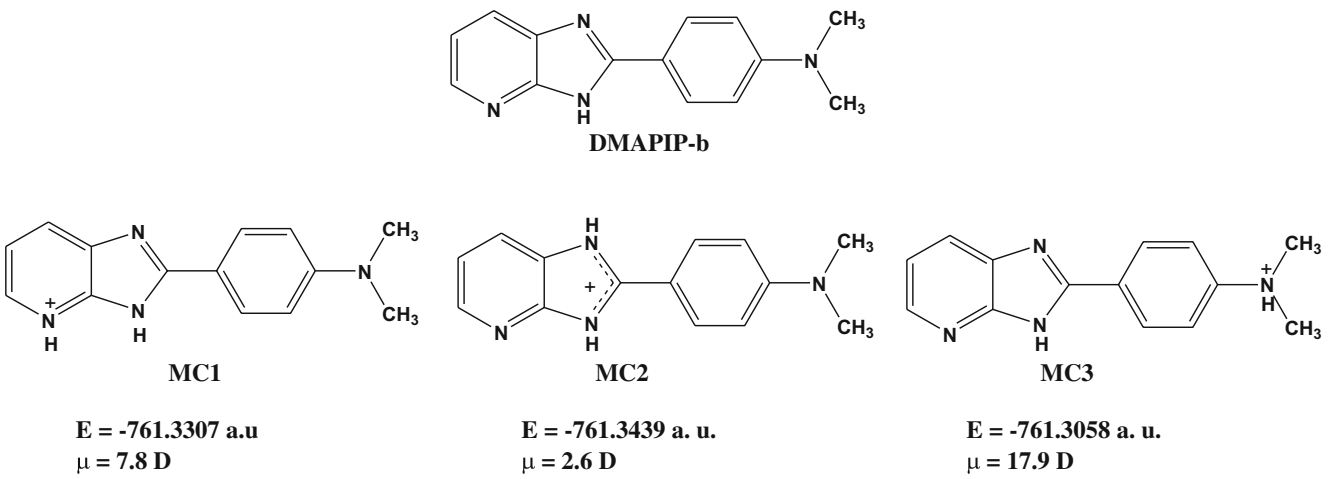

Scheme 1 DMAPIP-b and its monocations

of TX-100 (nonionic), CTAB (cationic) and SDS (anionic) micelles on the photophysics of DMAPIP-b. The studies result in an interesting observation that TICT emission is induced only in SDS and TX-100, but not in CTAB.

Materials and methods

DMAPIP-b was synthesized from 2, 3-diaminopyridine and 4-dimethylamino benzoic acid by the procedure reported in our previous paper [5]. TX-100 (Aldrich), CTAB (99%, Sigma) and SDS (≥99%, Sigma) were used as received. Millipore water was used for preparing aqueous solutions. The pH of the aqueous solutions was adjusted by addition of NaOH or H_2SO_4. Spectral measurements were performed at the solute concentration of 5×10^{-6} M. Absorption and fluorescence spectra were recorded on Cary 50 and Cary Eclipse instruments, respectively. Fluorescence spectra reported were corrected spectra. Fluorescence lifetimes were measured with the use of the Jobin Yon Spex Fluorocube instrument. IBH 375 nm LED was used for excitation and emission intensity was recorded using 420 nm Scotch cut-off filters. The Fluorocube instrument employs a TBX-04 detector with jitter timing of 250 ps FWHM or better. The fluorescence decays were analyzed with the reconvolution method using software provided by IBH. All experiments were performed at 300 K.

Results and discussion

Absorption and steady-state fluorescence

Spectral data of DMAPIP-b in micelles along with few solvents are compiled in Table 1. The longer wavelength absorption maximum is red shifted in micelle with small increase in molecular extinction coefficient. The spectral behaviors are consistent with the solublization of the molecule in micelles. Upon addition of surfactant, the fluorescence spectrum of DMAPIP-b is blue shifted with increase in intensity (Figs. 1, 2 and 3). But the difference between SDS and other surfactants is, SDS triggers dual emission in DMAPIP-b and two clear emission bands start to appear in SDS solution at concentrations above 4 mM. The intensity of the longer wavelength band increases with further increases in SDS concentration (Fig. 3). No such clear two band spectrum was observed in TX-100 or CTAB even at 40 mM solution. The overall fluorescence increases by a factor of 38 in TX-100, 36 in CTAB and 4.3 in SDS.

The spectral characteristics of DMAPIP-b have been studied well [5]. DMAPIP-b emits dual emission only in protic solvents. The shorter wavelength emission is from LE state. The longer wavelength emission is due to formation of a TICT state facilitated by the hydrogen bonding of the solvent with pyridine nitrogen of DMAPIP-b. The intensity ratio of the TICT to normal emission increases with increase in hydrogen bonding capacity of the solvent. But in water the TICT emission is almost completely quenched. This was attributed to greater stabilization of the highly polar TICT state by strong dipole-dipole and hydrogen bonding interactions with water, and consequently, rapid nonradiative transition to the ground and/or low lying triplet state. Based on the above results and considering results in the present study, the shorter wavelength band in SDS and the emission bands in CTAB and TX-100 can be assigned to normal emission and the longer wavelength emission band in SDS can be assigned to TICT emission.

Table 1 Absorption band maxima (λ_{max}[a], nm), log ϵ_{max}, M^{-1} cm^{-1}, fluorescence band maxima (λ_{max}[f], nm) and fluorescence life time (τ, ns) for neutral DMAPIP-b in different media

Medium	λ_{max}[a]	log ϵ_{max}	λ_{max}[f]	τ[1]
Cyclohexane	336, 352 (sh)	–	359, 379, 398	1.99
Acetonitrile	345	4.50	407	1.50
Ethanol	350	4.48	413	0.85 (21.05)
			494	2.07 (78.95)
Methanol	350	4.50	414	0.31 (56.50)
			506	1.16 (43.50)
Water (pH 9.0)	345	4.39	451	0.16 (98.75)
				2.13 (01.25)
SDS (50 mM, pH 10.2)	349	4.50	431	0.30 (70.18)
			530	1.25 (29.82)
TX-100 (80 mM, pH 7.3)	352	4.46	416	1.24 (91.31)
				3.06 (8.69)
CTAB (80 mM, pH 7.1)	353	4.45	424	1.30

[1] λ_{coll}>420 nm, figures in parenthesis show relative amplitudes

Binding constants of DMAPIP-b with different micelles have been determined following the method proposed by Almgren et al. [10]. According to the method

$$(F_m - F_0)\Big/(F_{in} - F_0) = 1 + (K[M])^{-1}$$

where, F_0, F_m and F_{in} are the fluorescence intensities of the probe in absence of surfactant, in micellar solutions of concentration [M], and under conditions of complete micellization respectively. *K* represents the binding constant between the probe in the excited state and micelle. The micellar concentration

$$[M] = ([S] - CMC)/n$$

where [S] is the surfactant concentration and *n* is the aggregation number. The aggregation numbers were taken as 143, 60 and 62 for TX-100, CTAB and SDS, respectively [11]. The binding constants obtained for TX-100, CTAB and SDS are $4.6\pm0.2\times10^4$, $3.3\pm0.4\times10^4$, and $5.1\pm0.8\times10^5 M^{-1}$ respectively.

Fluorescence lifetime

Fluorescence lifetime data obtained in different micelles along few solvents are listed in Table 1. Single exponential decays were observed in aprotic solvents. However two different lifetimes due to normal and TICT emissions were observed in protic solvents [5].The lifetime of the LE state is attenuated in protic solvents compared to aprotic solvents and the shortest lifetime is observed in water. The short lifetime of the normal emission in protic solvent may due to the strong intermolecular hydrogen bonding between DMAPIP-b and protic solvent molecules, resulting in an increase in the nonradiative decay rate of the LE state. Thus, as expected the lifetime of the normal emission increases in all the three micelles compared to water. Biexponential decays are observed in SDS and TX-100. This indicates that not only SDS micelle, TX-100 micelle also triggers the dual emission in DMAPIP-b and the weak TICT emission is burried underneath the strongly enhanced normal emission. In β-cyclodextrin environment also no clear band TICT emission was observed for DMAPIP-b,

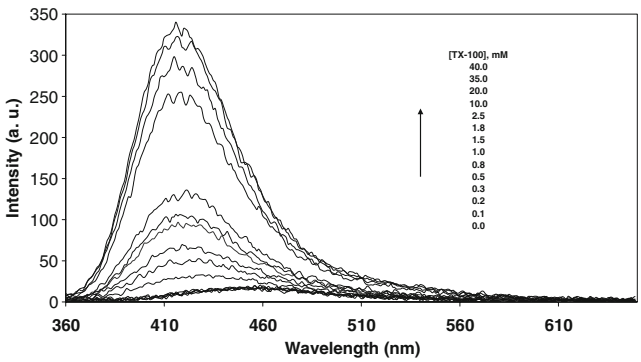

Fig. 1 Fluorescence Spectra of DMAPIP-b as a function of TX-100 concentration, λ_{exc}=350 nm

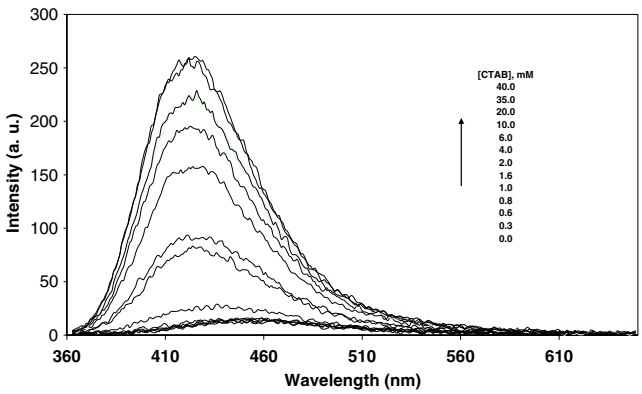

Fig. 2 Fluorescence Spectra of DMAPIP-b as a function of CTAB concentration (λ_{exc}=350 nm)

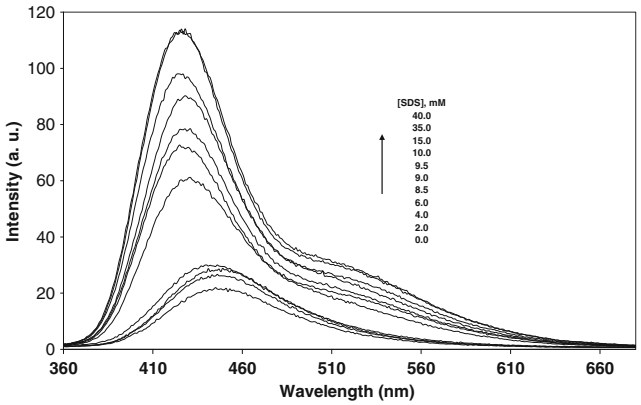

Fig. 3 Fluorescence Spectra of DMAPIP-b as a function of SDS concentration, λ_{exc}=350 nm

however biexponential decay clearly established the dual emission [12]. Monoexpoential decay of DMAPIP-b in CTAB, clearly suggests the absence of TICT emission in CTAB.

Nature of the binding site

Determination of polarity of the probe binding site inside the micelle has great importance in biological systems, and much attention has been drawn in that direction [13, 14]. In addition determination of micropolarity serves as an indicator of the local environment in which a given fluorophore is placed and enables one to find the probable location of the probe [15]. Single exponential decay for normal band and very high values of K establish that DMAPIP-b is present only at one site in the micelles. So we have made an attempt to evaluate the effective polarity at the micellar site of DMAPIP-b location from the correlation diagrams drawn between the fluorescence maxima of the normal band and $E_T(30)$, solvent polarity parameter [16] (not shown). The results clearly show that the micropolarity of DMAPIP-b binding sites in micelles, are close to that of alcohols. In other words, the probe molecule resides not in the core region, but in the micellar-water interface with limited exposures to water. The polarity experienced by the fluorophore in SDS is more compared to other micelles. This suggests that the amount of water molecules present in the Stern layer of SDS is more than the palisade region of TX-100 or the Stern layer of CTAB.

Kundu et al. proposed *p-N,N*-dimethylaminobenzonitrile present in SDS and CTAB with the dimethylamino group (donor) at the micellar periphery and the other end (acceptor) deep inside the micellar core [17]. On the other hand Jaffer et al. suggested two different orientation for TICT probe *trans*-2-[4-(dimethylamino)styryl]benzothiazole in SDS and CTAB. It was proposed that the $-NMe_2$ was oriented toward the micellar phase and the benzothiazole ring was projected toward the bulk aqueous environment in SDS and the orientation was reversed in CTAB [18]. It is well established that $-NR_2$ group acts as proton acceptor in the ground state [19]. The removal of water solvation shell around the $-NMe_2$ group would cause a red shift. The red shift in the absorption spectrum of DMAPIP-b in SDS indicates that $-NMe_2$ group is present in the micellar phase and the imidazopyridine ring is exposed to water. The orientation also ensures the hydrogen bonding of the water with pyridine nitrogen of DMAPIP-b and such a hydrogen bonding is necessary to induce the TICT emission in DMAPIP-b. The reduced polarities experienced by the molecule more destabilize the greater polar TICT state than the LE state. As a consequence, the energy of activation for the LE to TICT transition is increased, and hence increasing the normal emission [1, 2]. As far as the TICT state is concerned, destabilization inside the micellar environment increases the energy gap between the TICT state and the low lying states. This increase in energy gap reduces the nonradiative rate. This explains the observed TICT emission in SDS. In the reverse orientation, i.e. when imidazopyridine ring resides inside the micelle, the pyridine nitrogen is not available to form hydrogen bonding with water and may explain the absence of TICT emission in CTAB. However the red shift found in the absorption spectra of CTAB compared to water clearly rules out such an orientation for DMAPIP-b in CTAB. Thus the absence of TICT emission in CTAB and small TICT emission in TX-100 may be due to reduced hydrogen bonding experienced by the probe inside the micelle. Bagchi et al. also reported that the hydrogen bond donating capacity in micelles follows the order SDS > TX-100 > CTAB [20]. They also demonstrated that in SDS-TX-100 mixed micelle the hydrogen bonding donating ability decreases with increase in TX-100 concentration [21]. These properties in the micellar phase were attributed to the difference in extend of bound water molecules present in the micellar interface. Several other groups also observed that the environment of SDS is richer in water content as compared to that in TX-100 and CTAB [22, 23].

The large difference observed in the lifetimes of LE and TICT states in SDS and TX100 (Table 1), suggests that the equilibrium is not established between the two emitting states in these micelles also. The same behavior was reported for *p*-N,N-diethylamino benzoic acid in β-cyclodextrin [24]. It was shown that diethylamino group was located inside the cyclodextrin cavity and –COOH group outside the cavity, which was involved in hydrogen bonding, and increase in the rate of formation of TICT state and decrease in the rate of reverse process. A similar explanation can be offered in our case also, as the $-NMe_2$ group is projected toward the micellar core and the imidazopyridine ring towards the water rich part of the micelles. The shortest

lifetime observed for normal emission in SDS (among the micelles) substantiates the conclusion that DMAPIP-b experience a water rich environment inside SDS compared to TX-100 and CTAB.

pH effects

DMAPIP-b has three basic centers, but still only one absorption and one fluorescence bands correspond to the imidazole ring nitrogen protonated monocation was observed in aqueous medium [5]. It was reported that micelles strongly influence the formation and relative population of cations [25]. Since our present probe DMAPIP-b has three basic centers and it may form three types of monocations (Scheme 1): MC1 (protonation of pyridine nitrogen), MC2 (protonation of imidazole nitrogen) and MC3 (protonation of dimethylamino nitrogen). Thus we intend to know the effect of micelle on the protropic equilibrium. The absorption and fluorescence spectra of the dye at different pH were measured in CTAB (80 mM), TX-100 (80 mM), and SDS (50 mM) and the relevant data are along with the pK_a compiled in Table 2. Absorption spectra are red shifted in all the micelles with decrease in pH. The fluorescence maximum of DMAPIP-b in CTAB is red shifted with decrease in intensity with increase in acid concentration (Fig. 4). The behavior is also observed in TX-100 (Figure not shown). With decrease in pH the fluorescence normal band maximum in SDS is red shifted with increase in intensity and on the other hand the intensity of TICT band decreases (Fig. 5). These red shifts in absorption and fluorescence spectra are consistent with those observed in aqueous medium. But in micelle the fluorescence spectra are more complicated than in water. For example, in SDS at monocationic pH (the pH at which DMAPIP-b is completely present in monocationic form), a fluorescence band is observed at 435 nm with a long tail when λ_{exc}= 360 nm. With increase in λ_{exc} another band appears at longer wavelength side at 550 nm. The intensity ratio of the longer wavelength emission to shorter wavelength emission also increases with increase in λ_{exc} (Fig. 6). The behavior of the fluorescence excitation spectra also matches with emission spectra. Only one band (385 nm) is observed in the excitation spectrum when λ_{em}=430 nm and the band maxima shift

Table 2 Absorption band maxima ($\lambda_{max}{}^{a}$, nm), fluorescence excitation band maxima ($\lambda_{max}{}^{ex}$, nm) and emission band maxima ($\lambda_{max}{}^{f}$, nm) for monocationic DMAPIP-b and pK_a value in different media

Medium	$\lambda_{max}{}^{a}$	$\lambda_{max}{}^{ex}$	$\lambda_{max}{}^{f}$	pK_a
Water (pH 4.0)	386	–	451	5.4
CTAB (80 mM, pH 2.6)	379	360, 403	437, 530	3.6
TX-100 (80 mM, pH 2.9)	387	368, 403	428, 523	3.9
SDS (50 mM, pH 5.1)	394	385, 407	434, 550	7.3

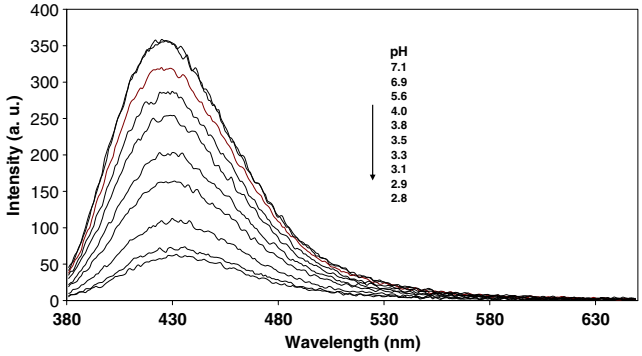

Fig. 4 Fluorescence spectra of DMAPIP-b in 80 mM CTAB as a function of pH, λ_{exc}=370 nm

towards red with increase in λ_{em}. At λ_{em}=610 nm the excitation spectral band appears at 407 nm (Fig. 7). These spectral behaviors are consistent with formation of two kinds of monocationic species in SDS. Similar excitation and emission spectral characteristics are also observed in TX-100 and CTAB at monocationic pH, and indicate the presence of two kinds of monocations in these micelles also (Table 2). The observed red shift in absorption and fluorescence spectra rules out the protonation of dimethylamino nitrogen. However a large red shift is expected in particular with the fluorescence spectrum due to TICT emission, on protonation of pyridine ring nitrogen [26]. Thus the longer wavelength excitation and emission spectral bands can be assigned to MC1 and the shorter wavelength excitation and emission ones to MC2.

To substantiate further, we have optimized the geometries of all the monocations in the ground state by density functional theory (DFT) [27] method using the hybrid Becke3 [28] and the Lee-Yang-Parr functionals [29] (B3LYP) in conjunction with 6-31G* basis set by Gaussian 03 W package to calculate the ground state energy and dipole moment. The results thus obtained are presented in Scheme 1. Theoretical calculations predicted MC2 as the most stable and least polar monocation. As mentioned earlier, only absorption and fluorescence bands correspond

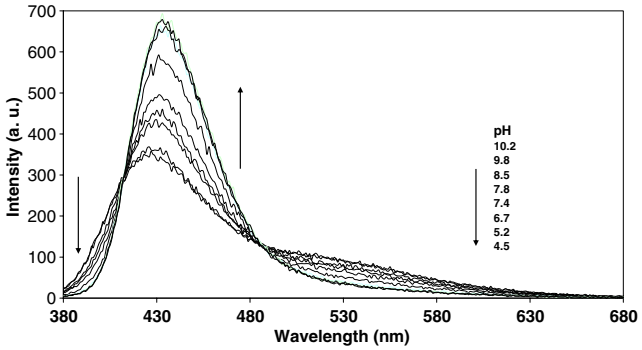

Fig. 5 Fluorescence spectra of DMAPIP-b in 50 mM SDS as a function of pH, λ_{exc} =370 nm

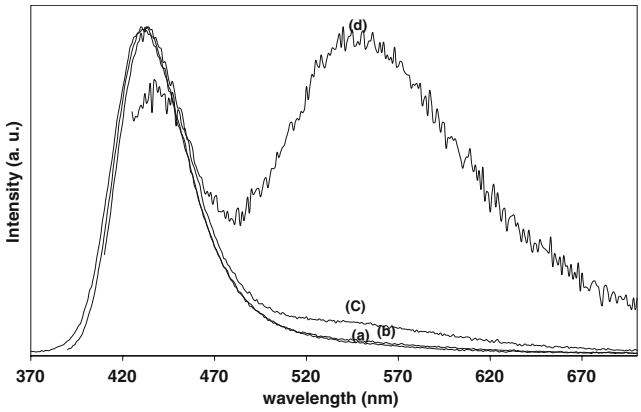

Fig. 6 Normalized fluorescence emission spectra of monocations of DMAPIP-b in SDS at (*a*) λ_{exc}=360 nm; (*b*) λ_{exc}=380 nm; (*c*) λ_{exc}= 400 nm; (*d*) λ_{exc}=420 nm

to MC2 was observed in aqueous medium [5]. The observation of MC1, in the less polar micellar media may be due to reduced nonradiative rates (like the TICT emission of neutral DMAPIP-b). The excitation energies were obtained by vertical excitations of optimized ground states using time dependent DFT (TDDFT) using B3LYP/6-31G calculations [30, 31]. The TDDFT excitation energies values for MC1 and MC2 are 2.50 eV and 3.39 eV respectively. The calculations also predict MC1 is more red shifted than MC2. The theoretical excitation energy obtained for MC2 (3.39 eV) is in very good agreement with experimental value (3.37 eV in TX-100). But the TDDFT excitation energy for MC1 is very small (2.50 eV) compared to experimental value (3.05 eV in TX-100). It is reported in the literature that TDDFT poorly describes some charge transfer situations, in which little or no overlap between the atomic orbitals contributing to the HOMO and those to the LUMO [32, 33]. However ZINDO calculations predict the excitation energy for MC1 as 2.89 eV and is in fair agreement with the experimental value (3.05 eV).

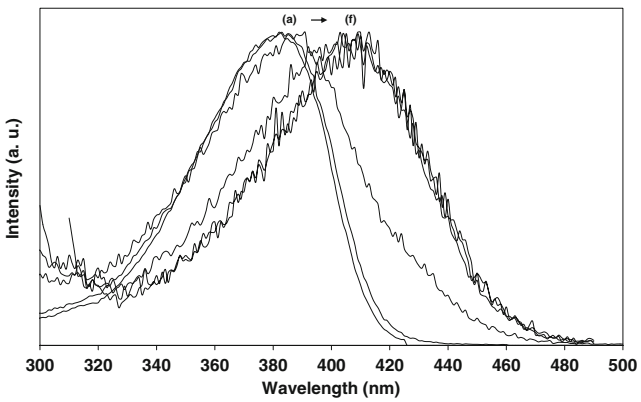

Fig. 7 Normalized fluorescence excitation spectra of monocations of DMAPIP-b in SDS at λ_{em}=430 nm; (*b*) λ_{em}=470 nm; (*c*) λ_{exc}= 510 nm; (*d*) λ_{em}=570 nm; (*e*) λ_{em}=590 nm; (*f*) λ_{exc}=610 nm

The striking difference between SDS and other micelles is the increase in fluorescence intensity with decrease of pH (Fig. 5). This could be due to large decrease in nonradiative rates for monocationic species than the neutral molecule in anionic micelle. In monocationic forms of the dye, imdazopyridine ring posses more positive charge and it interacts with the negative charge of the SDS polar head group. This results in higher binding between cation and SDS. In addition the dipole-dipole interaction attracts the imidazopyridine ring towards the Stern layer and pushes the rest of the cation more deep inside the micelle. This reduces the interaction of monocation with water.

Fluorescence spectra of the monocations were also studied as function of surfactant concentration. The fluorescence intensities of both the monocations increase with increase in surfactant concentration. The fluorescence intensities of both emission and excitation spectra of monocations are plotted against the surfactant concentrations to find the CMC of the surfactant and are compiled for in Table 3. The increase in the CMC of the nonionic micelles and the decrease in the CMC of the anionic micelle with the addition of protic acids is consistent with earlier works [22, 34, 35]. Interestingly the CMC value obtained for SDS using MC1 fluorescence intensities is lower than the value that obtained using MC2. This shows that MC1 has specific interaction with SDS and induces the formation of micelle at a lower concentration.

The apparent pK_a value is lower in TX-100 and CTAB than in water, but the apparent pK_a value is higher in SDS with respect to water (Table 2). Similar decrease in the pK_a value was reported for neutral-monocation equilibrium by others [22, 34] in TX-100 and is due to decrease in dielectric constant. A similar kind of explanation does not hold well for the apparent pKa value observed in SDS and CTAB and may be explained on the basis of a pseudo-phase ion-exchange (PIE) model [36, 37]. According to the model, in anionic micelle the protons and the cations tend to concentrate in the Stern layer and suppress the release of protons from the probe, resulting in an increase in apparent pK_a. In contrast, in cationic micelle positively charged species are repelled to the aqueous phase. To ensure that the increase in the apparent pKa value in SDS is only due to

Table 3 Critical micelle concentrations (CMC, mM) determined using emission and excitation intensities of different monocations

Micelle	MC1		MC2	
	Emission	Excitation	Emission	Excitation
SDS	0.9	1.0	3.3	3.5
TX-100	6.7	6.3	6.9	6.5
CTAB	1.9	1.7	1.6	1.8

the change in dielectric constant and potential (Ψ_0) at the surface, we have used the following relation [32]

$$pK_a^{obs} = pK_a^{i} - (e\Psi_0/2.303k_bT)$$

where pK_a^{obs} and pK_a^{i} are the apparent pK_a value for the acid–base indicator at the charged surface and for the interface if surface potential is zero, and e, k_b, and T are the charge on the electron, the Boltzmann constant, and the temperature in Kelvin, respectively. Taking the upper limit of surface potential equal to −140 mV for SDS [37] pK_a^{i} as 3.9 in TX-100, the pK_a^{obs} in SDS will be 6.3, which is much lower than that observed in SDS (7.3). This suggests that the higher value of the apparent pK_a value in SDS is due to the specific molecular interactions of DMAPIP-b with SDS, besides smaller dielectric constant and electrostatic potential.

Conclusion

DMAPIP-b resides in the micellar-water interface, while the $-NMe_2$ present inside the micellar phase, the imdazopyridine ring projected towards the micellar periphery. Of the micelles studied, DMAPIP-b emits dual fluorescence only in SDS and TX-100. The reduced polarity and the hydrogen bonding capacity experienced by the fluorophore inside micelles triggers the TICT emission in DMAPIP-b. The TICT emission is strong and emerges as a separate band in SDS, but in TX-100 it is weak and buried underneath the normal emission. The absence of TICT emission in CTAB is due to small hydrogen bond donating ability experienced by the molecule. Unlike water, the fluorescence from MC1 is also observed in micelle in addition to that from MC2. MC1 induces the micelle formation in SDS at lower concentration.

Acknowledgement The work is supported by Department of Science and Technology, New Delhi through funding the project SR/S1/PC-19/2006. The authors acknowledge Francis A. S. Chipem for performing some theoretical calculations for this work.

References

1. Rettig W (1986) Charge separation in excited-states of decoupled systems—TICT compounds and implications regarding the development of new lasers-dyes and the primary processes of vision and photosynthesis. Angew Chem Int Ed Engl 25:971–988
2. Grabowski ZR, Rotkiewicz K, Rettig W (2003) Structural changes accompanying intramolecular electron transfer: Focus on twisted intramolecular charge-transfer states and structures. Chem Rev 103(10):3899–4031
3. Bhattacharyya K, Chowdhury M (1993) Environmental and magnetic field effects on exciplex and twisted charge transfer emission. Chem Rev 93(1):507–535
4. Rettig W, Lapouyade R (1994) Fluorescence probes based on twisted intramolecular charge transfer states and other adiabatic photoreactions. In: Lakowicz JR (ed) Topics in fluorescence spectroscopy, probe design and chemical sensing, vol 4. Plenum Press, New York, pp 109–149
5. Dash N, Chipem FAS, Swaminathan R, Krishnamoorthy G (2008) Hydrogen bond induced twisted intramolecular charge transfer in 2-(4′-N, N-dimethylamino) phenylimidazo[4, 5-b]pyridine. Chem Phys Lett 460:119–124
6. Fendler JH (1982) Membrane mimetic chemistry. Wiley-Interscience, New York
7. Ramamurthy V (1991) Photochemistry in organized and constrained media. VCH, New York
8. Lopez F, Cuomo F, Ceglie A, Ambrosone L, Palazzo G (2008) Quenching and dequenching of pyrene fluorescence by Nucleotide Monophosphates in cationic micelles. J Phys Chem B 112 (24):7338–7344
9. Singh AK, Darshi M (2002) Fluorescence probe properties of intramolecular charge transfer diphenylbutadienes in micelles and vesicles. Biochim Biophys Acta 1563:35–44
10. Almgren M, Grieser F, Thomas JK (1979) Dynamic and static aspects of solubilization of neutral arenes in ionic micellar solutions. J Am Chem Soc 101(2):279–291
11. Saroja G, Ramachandan B, Saha S, Samanta A (1999) The fluorescence response of a structurally modified 4-aminophthalimide derivative covalently attached to a fatty acid in homogeneous and micellar environments. J Phys Chem B 103(15):2906–2911
12. Mohr A, Talbiersky P, Korth HG, Sustmann R, Boese R, Bläser D, Rehage H (2007) A new pyrene-based fluorescent probe for the determination of critical micelle concentrations. J Phys Chem B 111(45):12985–12992
13. Dash N, Chipem FAS, Krishnamoorthy G Unpublished results
14. Banerjee P, Pramanik S, Sarkar A, Bhattacharya SC (2008) Modulated photophysics of 3-pyrazolyl-2-pyrazoline derivative entrapped in micellar assembly. J Phys Chem B 112(24):7211–7219
15. Chakrabarty A, Das P, Mallick A, Chattopadhyay N (2008) Effect of surfactant chain length on the binding interaction of a biological photosensitizer with cationic micelles. J Phys Chem B 112(12):3684–3692
16. Kosower EM (1968) An introduction to physical organic chemistry. Wiley, New York
17. Kundu S, Maity S, Bera SC, Chattopadhyay N (1997) Twisted intramolecular charge transfer of dimethylaminobenzonitrile in micellar environments—a way to look at the orientation of the probe within the apolar microenvironment. J Mol Struct 405(2–3):231–238
18. Jaffer SS, Sowmiya M, Saha SK, Purkayastha P (2008) Defining the different phases of premicellar aggregation using the photophysical changes of a surface-probing compound. J Colloid Interface Sci 325(1):236–242
19. Krishnamoorthy G, Dogra SK (2000) Twisted intramolecular charge transfer of 2-(4′-N, N-dimethylaminophenyl)pyrido[3, 4-d] imidazole in cyclodextrins: Effect of pH. J Phys Chem A 104 (12):2542–2551
20. Shannigrahi M, Bagchi S (2004) Use of fluorescence probes for characterization of solvation properties of micelles: a linear solvation energy relationship study. J Phys Chem B 108 (46):17703–17708
21. Deb N, Shannigrahi M, Bagchi S (2008) Use of fluorescence probes for studying kamlet-taft solvatochromic parameters of micellar system formed by binary mixture of sodium dodecyl sulfate and Triton-X 100. J Phys Chem B 112(10):2868-2873.

22. Krishnamoorthy G, Dogra SK (1999) Twisted intramolecular charge transfer emission of 2-(4′-N, N-dimethylaminophenyl) benzimidazole in micelles. J Colloid Interface Sci 213(1):53–61
23. Gaber M, El-Daly SA, El-Sayed YS (2008) Spectral properties and inclusion of 3-(4′-dimethylaminophenyl)-1-(2-furanyl)prop-2-en-1-one in organized media of micellar solutions, beta-cyclodextrin and viscous medium. Colloid Surf B 66(1):103–109
24. Kim YH, Cho DW, Yoon M, Kim D (1996) Observation of hydrogen-bonding effects on twisted intramolecular charge transfer of p-(N, N-diethylamino)benzoic acid in aqueous cyclodextrin solutions. J Phys Chem 100(39):15670–15676
25. Krishnamoorthy G, Dogra SK (2000) Effect of micelles on the prototropic equilibrium of 2-(4′-N, N-dimethylaminophenyl) pyrido[3, 4-d]imidazole. Phys Chem Chem Phys 2(11):2521–2528
26. Krishnamoorthy G, Dogra SK (1999) Spectral characteristics of the various prototropic species of 2-(4′-N, N-dimethylaminophenyl) pyrido[3, 4-d]imidazole. J Org Chem 64(18):6566–6574
27. Kohn W, Sham LJ (1965) Self-consistent equations including exchange and correlation effects. Phys Rev A 140:1133–1138
28. Becke AD (1993) Density-functional thermochemistry .3. the role of exact exchange. J Chem Phys 98(7):5648–5652
29. Lee CT, Yang W, Parr RG (1988) Development of the Colle-Savetti correlation-energy formula into a functional of the electron-density. Phys Rev B 37(2):785–789
30. Casida ME (1995) In: Chong DP (ed) Recent Advances in Density Functional Methods, Part I. World Scientific, Singapore, p 155
31. Gross E, Dobson J, Petersilka M (1996) Top Curr Chem 181:81–172
32. Dreuw A, Weisman JL, Head-Gordon MJ (2003) Chem Phys 119:2943–2946
33. Sobolewski AL, Domcke W (2003) Chem Phys 294:73–83
34. Das SK, Dogra SK (1998) Excited state intramolecular proton transfer of 2-(2′-hydroxyphenyl)benzimidazole in non-ionic micelles: Brijs. J Chem Soc Faraday Trans I 94(1):139–145
35. Pandey S, Sarpal RS, Dogra SK (1995) Luminescence characteristics of 5-aminoindazole in cationic and anionic micelles at various pH. J Colloid Interface Sci 172(2):407–414
36. Drummond CJ, Grieser F, Healy TW (1989) Acid-base equilibria in aqueous micellar solutions. 1. Simple weak acids and bases. J Chem Soc Faraday Trans 1 85(3):521–535
37. Romsted LS, Zanethe D (1988) Quantitative treatment of indicator equilibria in micellar solutions of sodium decyl phosphate and sodium lauryl sulfate. J Phys Chem 92 (16):4690–4698